The Astrophysical Journal Letters, 739:L31 (6pp), 2011 September 20 doi:10.1088/2041-8205/739/1/L31

EXTENDED COLD MOLECULAR GAS RESERVOIRS IN $z \simeq 3.4$ SUBMILLIMETER GALAXIES

Dominik A. Riechers[1], Jacqueline Hodge[2], Fabian Walter[2], Christopher L. Carilli[3], and Frank Bertoldi[4]
[1] Astronomy Department, California Institute of Technology, MC 249-17, 1200 East California Boulevard, Pasadena, CA 91125, USA; dr@caltech.edu
[2] Max-Planck-Institut für Astronomie, Königstuhl 17, D-69117 Heidelberg, Germany
[3] National Radio Astronomy Observatory, P.O. Box O, Socorro, NM 87801, USA
[4] Argelander-Institut für Astronomie, Universität Bonn, Auf dem Hügel 71, D-53121 Bonn, Germany
Received 2011 April 14; accepted 2011 May 18; published 2011 August 29

ABSTRACT

We report the detection of spatially resolved CO($J = 1\rightarrow0$) emission in the $z \sim 3.4$ submillimeter galaxies (SMGs) SMM J09431+4700 and SMM J13120+4242, using the Expanded Very Large Array (EVLA). SMM J09431+4700 is resolved into the two previously reported millimeter sources H6 and H7, separated by ∼30 kpc in projection. We derive CO($J = 1\rightarrow0$) line luminosities of $L'_{\rm CO(1-0)} = (2.49 \pm 0.86)$ and $(5.82 \pm 1.22) \times 10^{10}$ K km s^{-1} pc^2 for H6 and H7, and $L'_{\rm CO(1-0)} = (23.4 \pm 4.1) \times 10^{10}$ K km s^{-1} pc^2 for SMM J13120+4242. These are ∼1.5–4.5 times higher than what is expected from simple excitation modeling of higher-J CO lines, suggesting the presence of copious amounts of low-excitation gas. This is supported by the finding that the CO($J = 1\rightarrow0$) line in SMM J13120+4242, the system with the lowest CO excitation, appears to have a broader profile and more extended spatial structure than seen in higher-J CO lines (which is less prominently seen in SMM J09431+4700). Based on $L'_{\rm CO(1-0)}$ and excitation modeling, we find $M_{\rm gas} = 2.0$–4.3 and 4.7–$12.7 \times 10^{10}\ M_\odot$ for H6 and H7, and $M_{\rm gas} = 18.7$–$69.4 \times 10^{10}\ M_\odot$ for SMM J13120+4242. The observed CO($J = 1\rightarrow0$) properties are consistent with the picture that SMM J09431+4700 represents an early-stage, gas-rich major merger and that SMM J13120+4242 represents such a system in an advanced stage. This study thus highlights the importance of spatially and dynamically resolved CO($J = 1\rightarrow0$) observations of SMGs to further understand the gas physics that drive star formation in these distant galaxies, which is possible only now that the EVLA is rising to its full capabilities.

Key words: cosmology: observations – galaxies: active – galaxies: formation – galaxies: high-redshift – galaxies: starburst – radio lines: galaxies

Online-only material: color figures

1. INTRODUCTION

With star formation rates of typically $>500\ M_\odot$ yr^{-1}, submillimeter galaxies (SMGs) are the most intense starbursts known at early cosmic times (see review by Blain et al. 2002). A significant fraction of the stellar mass assembly in massive galaxies at high redshift is thought to occur at early epochs ($z > 2$) on rapid timescales (<100 Myr) through a dusty, gas-rich SMG phase (e.g., Greve et al. 2005), making SMGs the likely progenitors of massive galaxies in the present-day universe.

A particularly useful probe for better understanding the physical conditions for star formation in these extreme starbursts is studies of the molecular interstellar medium that fuels the formation of stars. Dense molecular gas traced through CO was detected in 34 SMGs to date, typically revealing gas reservoirs of a few $10^{10}\ M_\odot$ (see the review by Solomon & Vanden Bout 2005). However, most of these detections are of CO rotational lines from $J \geqslant 3$ transitions, which may bias these studies toward highly excited gas, and do not necessarily trace the entire molecular gas reservoir as traced by CO($J = 1\rightarrow0$). Indeed, recent studies hint at the presence of substantial amounts of low-excitation gas in some SMGs (e.g., Hainline et al. 2006; Carilli et al. 2010; Harris et al. 2010; Ivison et al. 2010; Riechers et al. 2010b). Unfortunately, previous CO($J = 1\rightarrow0$) studies in SMGs (which do not suffer from excitation bias) were either carried out with single-dish telescopes lacking spatial information or with the old correlator of the Very Large Array lacking detailed spectral information.

To overcome the limitations of previous studies, we have initiated a systematic study of the CO($J = 1\rightarrow0$) content of SMGs and other galaxy populations with the Expanded Very Large Array (EVLA; Perley et al. 2011). Here we report early results for two $z \sim 3.4$ SMGs that appear to trace different stages of gas-rich, major mergers only ∼1.9 Gyr after the big bang. SMM J09431+4700 ($z = 3.346$) hosts two SMGs detected in $J \geqslant 4$ CO emission, separated by ∼30 kpc in projection, likely representing an early phase of a merger (e.g., Tacconi et al. 2006; Engel et al. 2010). SMM J13120+4242 ($z = 3.408$) shows a complex, disturbed structure in CO($J = 6\rightarrow5$), suggesting that it may represent an advanced-stage merger (Engel et al. 2010). We use a concordance, flat ΛCDM cosmology throughout, with $H_0 = 71$ km s^{-1} Mpc^{-1}, $\Omega_{\rm M} = 0.27$, and $\Omega_\Lambda = 0.73$ (Spergel et al. 2003, 2007).

2. OBSERVATIONS

We observed the CO($J = 1\rightarrow0$) ($\nu_{\rm rest} = 115.2712$ GHz) emission line toward SMM J09431+4700 and SMM J13120+4242, using the EVLA. At $z = 3.346$ and 3.408, this line is redshifted to 26.5235 and 26.1505 GHz (∼1.14 cm; K band). Observations were carried out under good weather conditions in the D array on 2010 May 19 and in the C array between 2010 December 16 and 2011 January 19, resulting in 4.0 hr (2.0 hr) total (on-source) observing time for SMM J09431+4700 (C array) and 7.5 hr (4.6 hr) for SMM J13120+4242 (C+D array). The nearby quasars J0920+4441 and J1312+4828 were observed every 4–7 minutes for pointing, secondary amplitude, and phase calibration. For primary flux calibration, the standard calibrator 3C286 was observed, leading to a calibration that is accurate within ∼10%. Observations were set up using a total

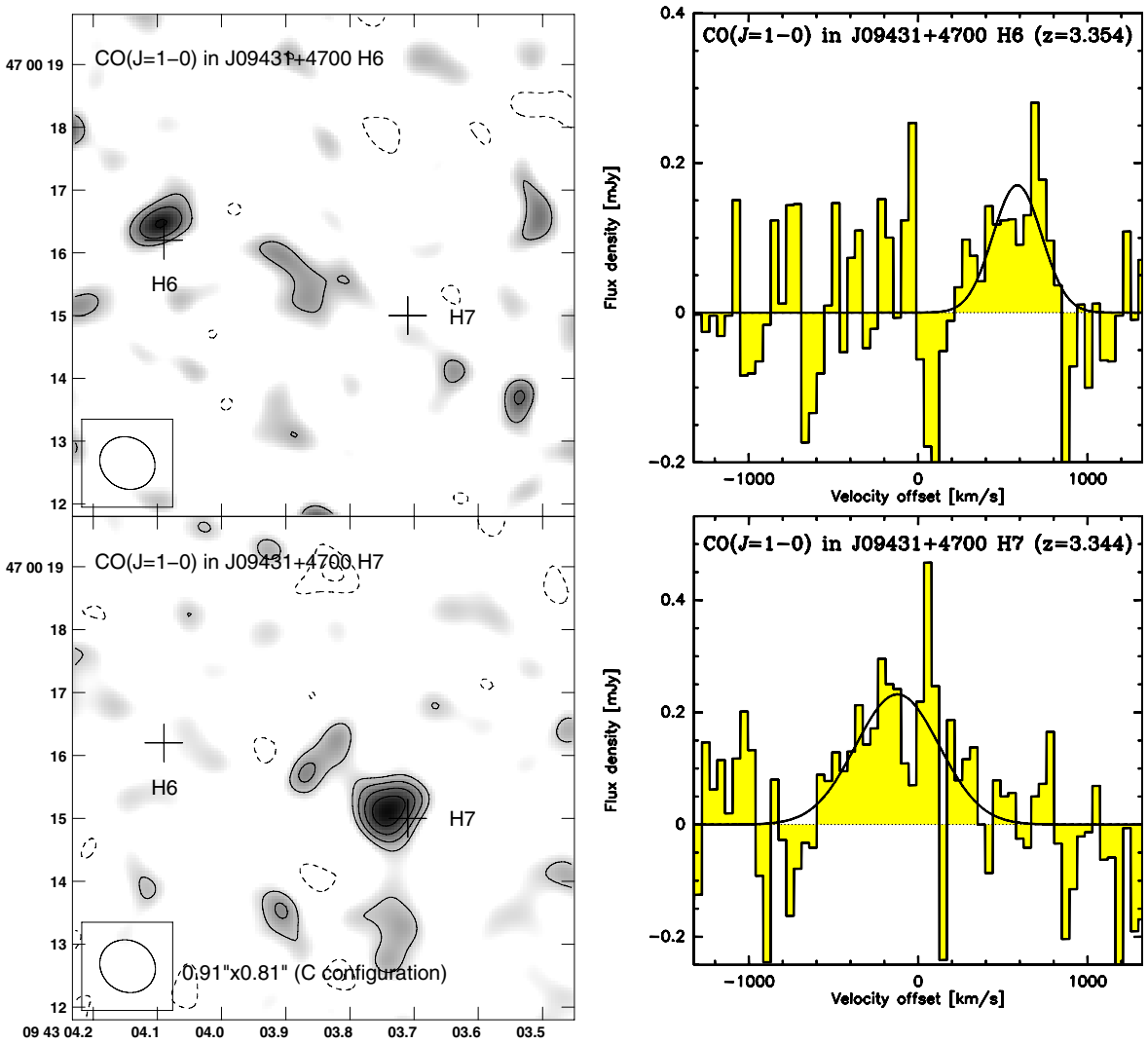

Figure 1. EVLA maps (left) and spectra (right) of CO($J = 1\rightarrow0$) emission toward the $z = 3.346$ SMG J09431+4700 H6 (top) and H7 (bottom). The resolution of both maps is $0\farcs91\times0\farcs81$. The crosses indicate continuum positions reported by Tacconi et al. (2006). Contours are shown in steps of $1\sigma = 30\,\mu$Jy beam^{-1}, starting at $\pm2\sigma$. The spectra (histograms) are shown at 45 km s^{-1} (4 MHz) resolution. Zero velocity corresponds to $z = 3.346$. The curves indicate Gaussian fits to the spectra. Top: emission toward H6, averaged over 475 km s^{-1} (42 MHz; central velocity: 585 km s^{-1}). Bottom: emission toward H7, averaged over 543 km s^{-1} (48 MHz; central velocity: -123 km s^{-1}).

(A color version of this figure is available in the online journal.)

bandwidth of 252 MHz (dual polarization; corresponding to ∼2900 km s^{-1} at 1.14 cm) with the WIDAR correlator.

For data reduction and analysis, the AIPS package was used. All data were mapped using "natural" weighting. The data result in a final rms of 105 and 70 μJy beam^{-1} per ∼45 km s^{-1} (4 MHz) channel for SMM J09431+4700 and SMM J13120+4242, respectively. Maps of the velocity-integrated CO $J = 1\rightarrow0$ line emission yield synthesized clean beam sizes of $0\farcs91\times0\farcs81$ and $1\farcs01\times0\farcs72$ at rms noise levels of 30 and 12 μJy beam^{-1} over 543 and 1513 km s^{-1} (48 and 132 MHz) for SMM J09431+4700 and SMM J13120+4242, respectively.

3. RESULTS

3.1. SMM J09431+4700

We detected spatially resolved CO($J = 1\rightarrow0$) emission toward SMM J09431+4700. The emission is resolved into two components that are separated by ∼30 kpc in projection, and are identified with the radio/millimeter continuum sources H6 and H7 (Figure 1). Component H7 appears marginally resolved at the ∼6.5 kpc resolution of our observations, suggesting an approximate source radius of 3 ± 1 kpc. This suggests that the CO($J = 1\rightarrow0$) line emission may be somewhat more extended than what is observed in higher-J lines (1.85 ± 0.60 and 1.13 ± 0.23 kpc in the CO $J = 4\rightarrow3$ and $6\rightarrow5$ lines; Engel et al. 2010). Component H6 appears unresolved at the moderate achieved signal-to-noise ratio. There is marginal evidence for some low surface brightness emission in between H6 and H7, but more sensitive observations are required to investigate this in more detail. We do not detect continuum emission toward either component down to a 3σ limit of 44 μJy beam^{-1} at 1.1 cm (rest frame 2.6 mm), consistent with the spectral energy distribution of this source.

From Gaussian fitting to the line profiles of H6 and H7, we obtain line peak strengths of $S_\nu = 170 \pm 58$ and $232 \pm 47\,\mu$Jy at line FWHMs of $\mathrm{d}v = 339 \pm 136$ and 580 ± 143 km s^{-1}, centered at redshifts of $z = 3.3545 \pm 0.0009$ and $z = 3.3442 \pm 0.0009$, respectively. The line widths correspond to 1.9× (H6) and 1.5× (H7) those measured in CO($J = 6\rightarrow5$) (Engel et al. 2010). The line parameters for H6 and H7 correspond to

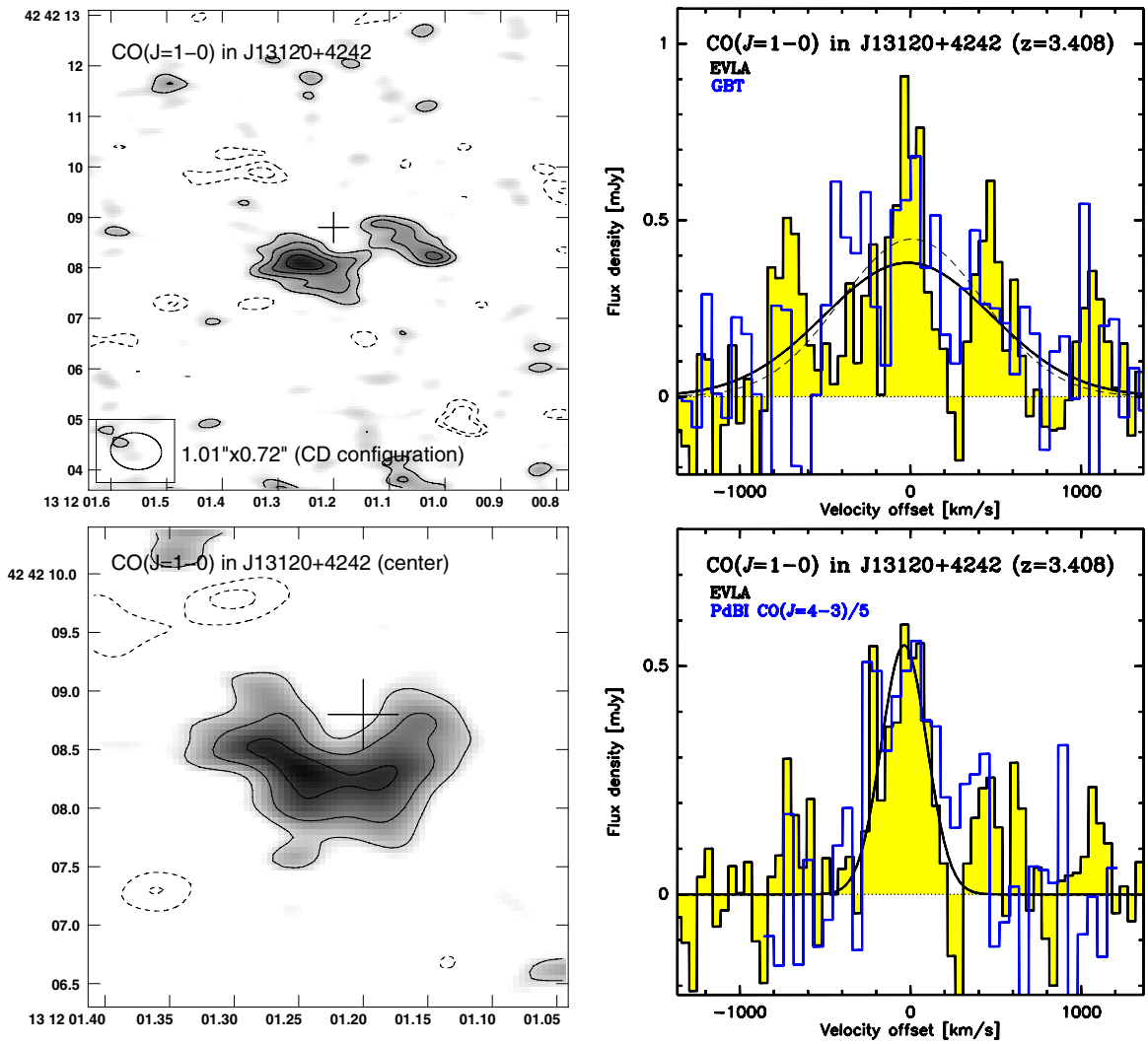

Figure 2. EVLA maps (left) and spectra (right) of CO($J = 1\rightarrow0$) emission toward the $z = 3.408$ SMG J13120+4242. The resolution of both maps is $1\farcs01\times0\farcs72$. The cross indicates the center of the CO($J = 4\rightarrow3$) emission detected at $\sim6''$ resolution (Greve et al. 2005). Contours are shown in steps of $1\sigma = 12$ and 29 μJy beam^{-1} (top/bottom), starting at $\pm2\sigma$. The spectra (histograms) are shown at 46 km s^{-1} (4 MHz) resolution and are extracted over the emission regions delimited by the 2σ contours in the maps to the left. Zero velocity corresponds to $z = 3.408$. The solid curves indicate Gaussian fits to the spectra. Top: total emission over 1513 km s^{-1} (132 MHz). The empty histogram and dashed curve in the right panel indicate the single-dish measurement with the Green Bank Telescope at $\sim28''$ resolution (Hainline et al. 2006). Bottom: emission over the central 344 km s^{-1} (30 MHz). The empty histogram shows the CO($J = 4\rightarrow3$) emission line, scaled down by a factor of 5 in flux density (Greve et al. 2005).

(A color version of this figure is available in the online journal.)

velocity-integrated emission line strengths of $I_{\rm CO(1-0)} = 0.061 \pm 0.021$ and 0.143 ± 0.030 Jy km s^{-1}, suggesting CO($J = 1\rightarrow0$) line luminosities of $L'_{\rm CO} = (2.49 \pm 0.86)$ and $(5.82 \pm 1.22) \times 10^{10}$ $(\mu_{\rm L}/1.2)^{-1}$ K km s^{-1} pc^2 (where $\mu_{\rm L} = 1.2$ is the lensing magnification factor; this SMG is located behind the galaxy cluster A851; Cowie et al. 2002).

3.2. SMM J13120+4242

We detected spatially resolved CO($J = 1\rightarrow0$) emission toward SMM J13120+4242. The emission peaks on a $(2\farcs0 \pm 0\farcs6) \times (0\farcs9 \pm 0\farcs4)$ $(15.0 \times 6.7$ kpc$^2)$ size region (Figure 2, bottom). The line profile averaged over this region is consistent with that seen in the CO($J = 4\rightarrow3$) line (empty histogram in Figure 2, bottom; Greve et al. 2005), and its complex morphological structure is consistent with what is seen in CO($J = 6\rightarrow5$) line emission (Engel et al. 2010). This component, however, carries only $\lesssim$40% of the observed CO($J = 1\rightarrow0$) line flux and appears to be embedded in a kinematically few times broader component that extends out to $\gtrsim2\times$ larger scales (Figure 2, top). The line profile over this whole extended structure appears to consist of multiple peaks. For consistency, we fit the line with a Gaussian profile, yielding $S_\nu = 380 \pm 65$ μJy and $dv = 1153 \pm 235$ km s^{-1}, and $I_{\rm CO(1-0)} = 0.464 \pm 0.081$ Jy km s^{-1}, centered at $z = 3.4078 \pm 0.0014$. Within the relative uncertainties, the line profile and parameters are consistent with a single-dish measurement of this line, carried out with the Green Bank Telescope at $28''$ resolution (empty histogram and dashed curve in Figure 2, top; Hainline et al. 2006). This suggests that the large apparent spatial extent of the CO($J = 1\rightarrow0$) emission is real and that virtually all line flux is recovered in the EVLA map. The line FWHM corresponds to $2.2\times$ and $1.3\times$ those measured in the CO($J = 4\rightarrow3$) and CO($J = 6\rightarrow5$) lines. We do not detect any rest-frame 2.6 mm continuum emission down to a 3σ limit of 60 μJy beam^{-1}, consistent with the spectral energy distribution of this source. Averaged over

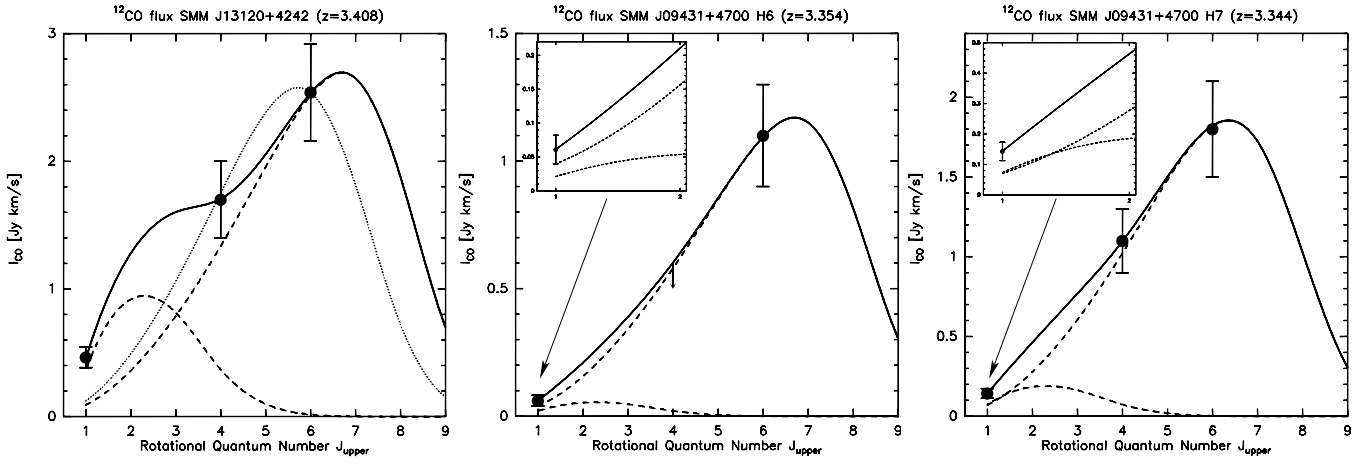

Figure 3. CO excitation ladders (points) and LVG models (lines) for SMM J13120+4242 and SMM 09431+4700 H6 and H7. The CO($J = 4\rightarrow3$) and CO($J = 6\rightarrow5$) data are adopted from Greve et al. (2005), Tacconi et al. (2006), and Engel et al. (2010). The insets show zoomed-in versions of the model fits close to the CO($J = 1\rightarrow0$) line. The data for all sources are well fitted by two-component LVG models, as indicated by the solid lines. The dashed lines indicate the two components of each model, represented by a low-excitation component with a kinetic temperature of $T_{\rm kin} = 25$ K and a gas density of $\rho_{\rm gas} = 10^{2.5}$ cm^{-3}, and a high-excitation component with $T_{\rm kin} = 40$ K and a gas density of $\rho_{\rm gas} = 10^{4.3}$ cm^{-3} (this component has a 1.26× lower $\rho_{\rm gas}$ for H7). The high-excitation components contribute 20%, 65%, and 49% to the observed CO($J = 1\rightarrow0$) intensities. For comparison, the dotted line in the left panel shows a single-component fit to the $J > 1$ lines with $T_{\rm kin} = 40$ K and $\rho_{\rm gas} = 10^{4.0}$ cm^{-3}.

the full region where CO($J = 1\rightarrow0$) line emission is detected, this suggests a conservative 3σ limit of $\sim$270 μJy. From the line intensity, we derive $L'_{\rm CO} = (23.4 \pm 4.1) \times 10^{10}$ K km s^{-1} pc^2.

4. ANALYSIS

4.1. Line Excitation Modeling

Besides the EVLA CO($J = 1\rightarrow0$) observations presented here, SMM J09431+4700 and SMM J13120+4242 were studied in CO($J = 4\rightarrow3$) and CO($J = 6\rightarrow5$) line emission (see Engel et al. 2010 for a summary of previous studies). Based on the observed CO excitation ladders, we can constrain the line radiative transfer through large velocity gradient (LVG) models, treating the gas kinetic temperature and density as free parameters. For all calculations, the H_2 ortho-to-para ratio was fixed to 3:1, the cosmic microwave background temperature was fixed to 11.84 and 12.01 K (at $z = 3.346$ and 3.408), and the Flower (2001) CO collision rates were used. We adopted a CO abundance per velocity gradient of $[{\rm CO}]/(dv/dr) = 1\times10^{-5}$ pc (km s^{-1})$^{-1}$ (e.g., Weiß et al. 2005a, 2007; Riechers et al. 2006). Components H6 and H7 of SMM J09431+4700 are fitted individually.

The sources are poorly fitted by single-component models, which underpredict the observed CO($J = 1\rightarrow0$) fluxes by factors of $\sim$1.5–4.5 when fitted to the higher-J lines.[5] The data for all sources can be fitted reasonably well with two gas components, which are represented by a "diffuse," low-excitation component with a kinetic temperature of $T_{\rm kin} = 25$ K and a gas density of $\rho_{\rm gas} = 10^{2.5}$ cm^{-3}, and a more "dense," high-excitation component with $T_{\rm kin} = 40$ K (comparable to the dust temperature in SMM J13120+4242; Kovács et al. 2006) and $\rho_{\rm gas} = 10^{4.3}$ cm^{-3} in our models ($\rho_{\rm gas} = 10^{4.2}$ cm^{-3} is used for H7, as it provides a slightly better fit). The two gas components differ in relative strength between the sources (Figure 3). For H6 and H7, we find that the dense gas components have surface filling factors of 13% and 7% relative to the low-excitation component. For SMM J13120+4242, we find that only $\sim$2% of the surface area associated with emission from the low-excitation component also shows emission from the dense gas component. This suggests that only a small fraction of the volume in these galaxies occupied by gas is associated with dense regions. Also, these model parameters suggest that the low-excitation gas components fill a dominant fraction of the area over which the sources are resolved in these observations.

The physical properties of the low-excitation gas components in these models are comparable to those of the gas in nearby spiral galaxies and "normal" high-z star-forming galaxies (e.g., Dannerbauer et al. 2009) and the low-excitation components found in other SMGs (e.g., Carilli et al. 2010; Riechers et al. 2010b). The properties of the high-excitation components are also comparable to what is found in other SMGs, ultraluminous infrared galaxy (ULIRG) nuclei, and high-z FIR-luminous quasars (e.g., Riechers et al. 2006, 2009; Weiß et al. 2005b). However, it appears that the relative fractions of low- and high-excitation gas differ between individual systems, perhaps due to different evolutionary stages.

4.2. Gas Masses and Surface Densities, Dynamical Masses, and Gas Mass Fractions

Based on the observed CO($J = 1\rightarrow0$) line luminosities, we can derive the total masses of the gas reservoirs in our targets. For SMGs, a ULIRG-like conversion factor of $\alpha_{\rm CO} = M_{\rm gas}/L'_{\rm CO} = 0.8\,M_\odot$ (K km s^{-1} pc^2)$^{-1}$ is commonly adopted (e.g., Downes & Solomon 1998; Tacconi et al. 2008). This suggests $M_{\rm gas} = 2.0$ and 4.7×10^{10} $(\mu_{\rm L}/1.2)^{-1}\,M_\odot$ for SMM J09431+4700 H6 and H7, and $M_{\rm gas} = 18.7\times10^{10}\,M_\odot$ for SMM J13120+4242, respectively. However, a low, ULIRG-like conversion factor may not be appropriate for the low-excitation gas components suggested by our models. Assuming $\alpha_{\rm CO} = 3.5\,M_\odot$ (K km s^{-1} pc^2)$^{-1}$ for these components (as suggested for gas components with comparable excitation found in disk-like high-z galaxies; e.g., Daddi et al. 2010), we find $M_{\rm gas} = 4.3$ and 12.7×10^{10} $(\mu_{\rm L}/1.2)^{-1}\,M_\odot$ for SMM J09431+4700 H6 and H7, and $M_{\rm gas} = 69.4\times10^{10}\,M_\odot$ for SMM J13120+4242, respectively.

[5] Given the limited constraints on H6, this source can be marginally fitted with a single component.

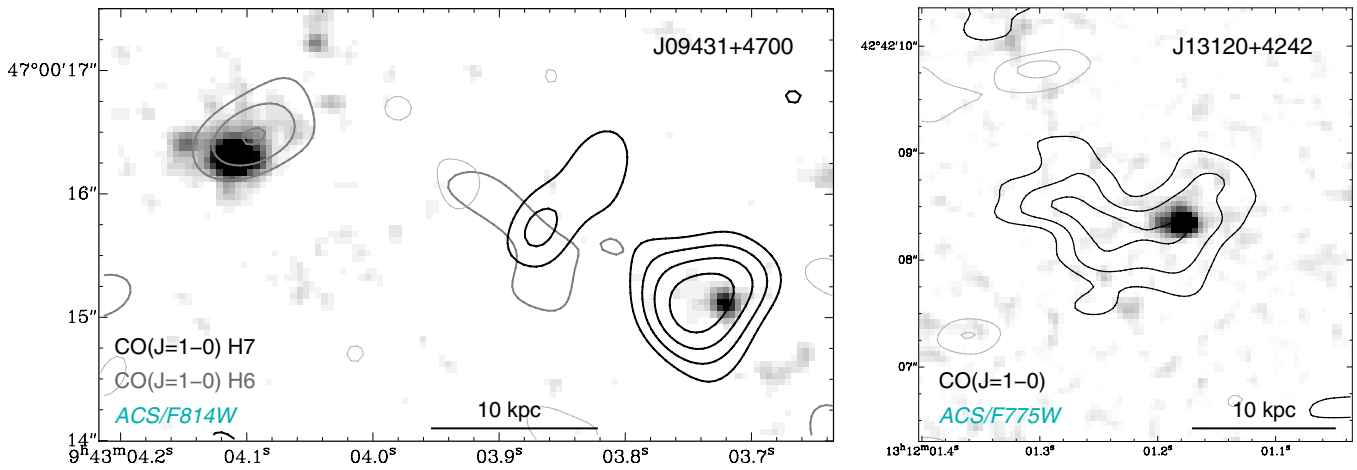

Figure 4. Overlays of the CO($J = 1\rightarrow0$) emission (contours, as in Figures 1 and 2) toward J09431+4700 (left) and the center of J13120+4242 (right) on *Hubble Space Telescope* ACS F814W (McGrath et al. 2008) and F775W images (gray scale; rest-frame ∼180 nm; smoothed with a 0.″1 Gaussian kernel; Hainline et al. 2006). The gray and black contours in the left panel indicate the velocity ranges for H6 and H7 as in Figure 1.

(A color version of this figure is available in the online journal.)

Assuming FWHM radii of 3 kpc for SMM J09431+4700 H6 and H7, the gas masses correspond to average gas surface densities of $\Sigma_{\rm gas}$ = 700–1500 and 1600–4500 $M_\odot$ pc^{-2}. The CO($J = 1\rightarrow0$) emission in SMM J13120+4242 is distributed over a projected area of ∼200 kpc^2, corresponding to $\Sigma_{\rm gas}$ = 960–3600 $M_\odot$ pc^{-2}.

SMM J13120+4242 has a stellar mass of $M_\star$ = 10.2–13.5×10^{10} $M_\odot$ (Engel et al. 2010). This yields a baryonic gas mass fraction of $f_{\rm gas}^{\rm bary} = M_{\rm gas}/(M_{\rm gas}+M_\star) = 0.58$–0.87, where the spread of values represents the difference in conversion factors as outlined above.

Using the "isotropic virial estimator" (e.g., Tacconi et al. 2008; Engel et al. 2010), we can also estimate the dynamical masses of our targets. Assuming FWHM radii of 3 kpc for SMM J09431+4700 H6 and H7, we find $M_{\rm dyn}$ = 9.7 and 28.3×10^{10} $M_\odot$, respectively. This corresponds to gas mass fractions $f_{\rm gas} = M_{\rm gas}/M_{\rm dyn}$ = 0.21–0.45 and 0.16–0.45 for H6 and H7, where the spread of values represents the use of different conversion factors as outlined above. This lies within the typical range of values estimated for SMGs (e.g., Tacconi et al. 2006, 2008). The CO($J = 1\rightarrow0$) emission in SMM J13120+4242 is spread over an area with a characteristic radius of 7.9 kpc. Assuming that the multiple peaks can be described by a single potential that is represented correctly by the FWHM on the Gaussian fit used above, we find $M_{\rm dyn}$ = 290×10^{10} $M_\odot$ for SMM J13120+4242. This corresponds to $f_{\rm gas}$ = 0.06–0.24. Under the assumption that the system is gravitationally bound, and that $M_{\rm gas}$+$M_\star$ corresponds to the bulk of baryonic matter in this system (the contributions of dust and black hole mass are expected to be minor), this would imply that this SMG is dominated by dark matter. However, given the complex velocity structure of this system, we consider it likely that $M_{\rm dyn}$ is overestimated by a factor of two to three with this simplified approach. Thus, we consider the gas fraction for SMM J13120+4242 a lower limit.

4.3. Origin of the Molecular Line Emission

SMM J13120+4242 and both components of SMM J09431+4700 are associated with galaxies detected with the *Hubble Space Telescope* in rest-frame optical/ultraviolet light (Figure 4). H7, the more CO-luminous component of SMM J09431+4700, is not significantly detected in *R*-band images of this source (Tacconi et al. 2006), which may indicate that it is more obscured than H6. The CO emission centroids in H6 and H7 are offset by ∼1.5 kpc (0.″2) from the centers of the optical emission, but are clearly associated with fainter, potentially more obscured regions in the galaxies. The optical emission in SMM J13120+4242 appears to be associated with one of the CO peaks in the central region, and thus, potentially with one component of a major merger (or a region of low dust obscuration).

5. DISCUSSION

We have detected spatially resolved CO($J = 1\rightarrow0$) emission toward the $z \sim 3.4$ SMGs SMM J09431+4700 and SMM J13120+4242. We resolve the gas reservoirs down to $\lesssim$5 kpc scales (given the sizes of our synthesized beams). CO($J = 1\rightarrow0$) emission in SMM J09431+4700 is detected toward both radio/millimeter continuum sources H6 and H7, which have been detected in higher-*J* CO lines in earlier work. There is marginal evidence for additional CO($J = 1\rightarrow0$) emission in between the two sources, which are separated by ∼30 kpc in projection. This, and their proximity in redshift (d$z \lesssim 0.01$), is consistent with the picture that this SMG is undergoing an early stage massive, gas-rich merger (see also Engel et al. 2010). The CO($J = 1\rightarrow0$) line in H7, the more CO-luminous component, appears to show a ∼50% larger line width and size relative to what is measured in higher-*J* CO lines, but the values are marginally consistent within the relative uncertainties.

The CO($J = 1\rightarrow0$) emission in SMM J13120+4242 shows a bright central peak that appears to be associated with the emission that dominates the flux in higher-*J* CO lines. It also shows >2 times broader emission (as also seen in single-dish observations at low spatial resolution; Hainline et al. 2006) distributed over several peaks that extends out to >15 kpc scales, but appears to be faint in higher-*J* CO lines. Thus, the EVLA CO($J = 1\rightarrow0$) observations reveal a spatially resolved CO excitation gradient in this SMG. This may suggest that this SMG is in an advanced stage of a merger, where the warm and dense, highly excited gas component predominantly arises from a starburst in the "overlap" region of two gas-rich galaxies, and the broader, more extended, less highly excited gas is associated

with tidal structure redistributed by the merger. More sensitive observations are required to study the dynamical structure of this complex system in more detail.

The CO($J = 1 \rightarrow 0$) properties of SMM J13120+4242 contrast those of high-z quasars, which appear to be dominated by less extended ($\sim$5 kpc), highly excited molecular gas reservoirs, with only little evidence for low-excitation gas (e.g., Riechers et al. 2006, 2009, 2011a; Weiß et al. 2007). They also contrast those of lensed $z \sim 3$ Lyman-break galaxies, which typically have an order of magnitude less massive, compact ($\sim$1–2 kpc) CO($J = 1 \rightarrow 0$) reservoirs (Riechers et al. 2010a; see also higher-J CO observations by Baker et al. 2004; Coppin et al. 2007). Massive, gas-rich star-forming galaxies can host gas reservoirs comparable in extent to those found in our target SMGs, but their spatial and velocity structure typically appears more symmetric and ordered (e.g., Daddi et al. 2010). Also, their overall CO excitation appears to be lower (Dannerbauer et al. 2009; Aravena et al. 2010). Low CO excitation was also found in the $z = 1.44$ SMG HR10, which was initially selected as an extremely red object (Andreani et al. 2000; Papadopoulos & Ivison 2002; Greve et al. 2003).

The new CO($J = 1 \rightarrow 0$) observations of the $z \sim 3.4$ SMGs SMM J09431+4700 and SMM J13120+4242 provide supporting evidence that they represent early and advanced stage, gas-rich major mergers. Recent, lower resolution CO($J = 1 \rightarrow 0$) studies of the $\sim$20 kpc separation merger SMM J123707+6214 ($z = 2.488$; Ivison et al. 2011; Riechers et al. 2011b) may suggest an intermediate merger stage (with two separated components, but closer in projected distance and redshift than in SMM J09431+4700), in between those observed in these two targets. These EVLA observations thus may be a first step toward establishing a molecular gas-based "merger sequence" for gas-rich starburst galaxies at high redshift, which may crucially constrain formation models of SMGs (e.g., Davé et al. 2010; Hayward et al. 2011).

If the CO($J = 1 \rightarrow 0$) properties of the $z \sim 3.4$ systems studied here are representative of their parent population, SMGs in advanced merger stages exhibit substantially more extended, broader low-J CO line emission than in earlier merger stages. Observations of high-J CO line emission alone will underestimate the gas content and extent of the tidal structure in advanced-stage mergers, yielding an incomplete picture of the processes that drive the gas dynamics in such systems.

The observations presented here thus show the key importance of spatially and dynamically resolved CO($J = 1 \rightarrow 0$) observations of SMGs to understand the gas physics that drive star formation in these luminous, massive gas-rich high redshift galaxies. In combination with higher-J CO line observations with shorter wavelength interferometers such as the upcoming ALMA, this makes the EVLA a uniquely powerful tool to distinguish different high-z galaxy populations based on their molecular gas content.

We thank the referee, Dr. Laura Hainline, for a helpful report, and Christian Henkel for the original version of the LVG code. D.R. acknowledges support from NASA through a *Spitzer Space Telescope* grant. The National Radio Astronomy Observatory is a facility of the National Science Foundation operated under cooperative agreement by Associated Universities, Inc.

REFERENCES

Andreani, P., Cimatti, A., Loinard, L., & Röttgering, H. 2000, A&A, 354, L1
Aravena, M., Carilli, C., Daddi, E., et al. 2010, ApJ, 718, 177
Baker, A. J., Tacconi, L. J., Genzel, R., et al. 2004, ApJ, 604, 125
Blain, A. W., Smail, I., Ivison, R. J., et al. 2002, Phys. Rep., 369, 111
Carilli, C. L., Daddi, E., Riechers, D., et al. 2010, ApJ, 714, 1407
Coppin, K., Swinbank, A. M., Neri, R., et al. 2007, ApJ, 665, 936
Cowie, L. L., Barger, A. J., & Kneib, J.-P. 2002, AJ, 123, 2197
Daddi, E., Bournaud, F., Walter, F., et al. 2010, ApJ, 713, 686
Dannerbauer, H., Daddi, E., Riechers, D. A., et al. 2009, ApJ, 698, L178
Davé, R., Finlator, K, Oppenheimer, B., et al. 2010, MNRAS, 404, 1355
Downes, D., & Solomon, P. M. 1998, ApJ, 507, 615
Engel, H., Tacconi, L. J., Davies, R. I., et al. 2010, ApJ, 724, 233
Flower, D. R. 2001, J. Phys. B: At. Mol. Opt. Phys., 34, 2731
Greve, T. R., Ivison, R. J., & Papadopoulos, P. P. 2003, ApJ, 599, 839
Greve, T. R., Bertoldi, F., Smail, I., et al. 2005, MNRAS, 359, 1165
Hainline, L. J., Blain, A. W., Greve, T. R., et al. 2006, ApJ, 650, 614
Harris, A. I., Baker, A. J., Zonak, S. G., et al. 2010, ApJ, 723, 1139
Hayward, C. C., Keres, D., Jonsson, P., et al. 2011, ApJ, submitted (arXiv:1101.0002)
Ivison, R. J., Papadopoulos, P. P., Smail, I., et al. 2011, MNRAS, 412, 1913
Ivison, R. J., Smail, I., Papadopoulos, P. P., et al. 2010, MNRAS, 404, 198
Kovács, A., Chapman, S. C., Dowell, C. D., et al. 2006, ApJ, 650, 592
McGrath, E. J., Stockton, A., Canalizo, G., Iye, M., & Maihara, T. 2008, ApJ, 682, 303
Papadopoulos, P. P., & Ivison, R. J. 2002, ApJ, 564, L9
Perley, R. A., Chandler, C. J., Butler, B. J., & Wrobel, J. M. 2011, ApJ, 739, L1
Riechers, D. A., Capak, P. L., Carilli, C. L., et al. 2010b, ApJ, 720, L131
Riechers, D. A., Carilli, C. L., Maddalena, R. J., et al. 2011a, ApJ, 739, L32
Riechers, D. A., Carilli, C. L., Walter, F., & Momjian, E. 2010a, ApJ, 724, L153
Riechers, D. A., Carilli, L. C., Walter, F., et al. 2011b, ApJ, 733, L11
Riechers, D. A., Walter, F., Bertoldi, F., et al. 2009, ApJ, 703, 1338
Riechers, D. A., Walter, F., Carilli, C. L., et al. 2006, ApJ, 650, 604
Solomon, P. M., & Vanden Bout, P. A. 2005, ARA&A, 43, 677
Spergel, D. N., Bean, R., Doré, O., et al. 2007, ApJS, 170, 377
Spergel, D. N., Verde, L., Peiris, H. V., et al. 2003, ApJS, 148, 175
Tacconi, L. J., Genzel, R., Smail, I., et al. 2008, ApJ, 680, 246
Tacconi, L. J., Neri, R., Chapman, S. C., et al. 2006, ApJ, 640, 228
Weiß, A., Downes, D., Neri, R., et al. 2007, A&A, 467, 955
Weiß, A., Downes, D., Walter, F., & Henkel, C. 2005b, A&A, 440, L45
Weiß, A., Walter, F., & Scoville, N. Z. 2005a, A&A, 438, 533